Solution of the radiative transfer equation for vertically inhomogeneous media by numerical integration solvers: comparative analysis

Ivan Chuprov, Daniil Konstantinov, Dmitry Efremenko, Vyacheslav Zemlyakov, Jiexing Gao

[1] Syktyvkar State University
[2] Moscow Institute of Physics and Technology (national research university)
[3] German Aerospace Center (DLR), Remote Sensing Technology Institute (IMF)

An efficiency of the singular value decomposition (SVD) method and ordinary differential equation (ODE) solvers in finding the reflection matrix are compared. A reflection matrix can be found by solving the one-dimensional radiative transfer equation. The latter's solution based on the discrete ordinate method leads to the singular value decomposition (SVD) method. Alternative approach consists in transforming the original problem into a matrix Riccati equation written specifically for the reflection matrix. The matrix Riccati equation is solved using numerical integration techniques for ordinary differential equations (ODEs). It is found that for a single layer case, the SVD approach is faster than the ODE solvers by an order of magnitude. Yet as the number of layers increases, the ODE solvers become more efficient than the SVD approach. In addition, they outperform the SVD method when a solution for a set of optical thicknesses of the medium should be found or when retrieval of optical thickness should be performed. The comparison between different ODE solvers is performed, as well.

Keywords: Radiative transfer equation; Riccati equation; ODE solvers

1 Introduction

The radiative transfer is an important issue for astrophysics and engineering sciences. The radiative transfer equation (RTE) describes the radiance field taking into account the multiple scattering process occurring inside the turbid medium. Several numerical methods were developed to solve the RTE (including the Monte-Carlo method, the spherical harmonics method and various analytical models) which date back to the XX century (see, e.g., [1-10] and references therein for a general review). The discrete ordinate method [11-13] is based on replacing the continuous dependence of the radiance on direction by a dependence on a discrete set of directions (the so called discrete ordinates). For a homogeneous layer, the discretized radiative transfer equation can be converted into a system of linear first-order ordinary differential equations (ODE). The solution of the ODE system can be expressed as a linear combination of characteristic solutions of the discretized problem, while in the matrix exponential formulation the solution is found by analytical integration of ODEs [14]. In both cases, the singular value decomposition (SVD) of the layer matrix incorporating the scattering properties of the layer should be performed, which is relatively time consuming step in the whole algorithm, as shown in [15-17].

Another approach involves the concept of invariant imbedding, which is due to Ambartsumian [18]. The invariant imbedding principle is based on the fact that the reflection function remains unchanged upon addition of a new layer. In Refs. [19, 20] it was showed that the reflection function derived by using the invariant imbedding satisfies the matrix Riccati equation.

If the medium is inhomogeneous, it can be represented as a set of homogeneous layers and then, the reflection and transmission matrices for all layers can be combined into the reflection and transmission matrices for a stack of layers using the matrix operator method [21] which involves the matrix multiplications and inversions.

The numerical integration of the matrix Riccati equation does not use the SVD step or the matrix operator method in the case of a inhomogeneous medium. On the other hand, once the SVD is performed, the rest computations are made analytically and do not involve any approximations, whereas the ODE solvers are based on approximate differential schemes and can be not efficient for stiff problems. In this regard, our goal in this paper is to compare efficiencies of SVD and ODE approches for solving one-dimensional RTE. The rest of the paper is organized as follows. In Section 2 we briefly expose the mathematical background of the SVD method and outline the transformation of the RTE into the matrix Riccati equation. In Section 3 we overview the ODE solvers chosen for the comparison. Section 4 presents the numerical simulations. The paper is concluded with a short summary.

2 Theory

2.1 The singular value decomposition approach

We consider a one-dimensional RTE for the radiance L:

$$\mu \frac{dL(\tau,\mu,\varphi)}{d\tau} = -L(\tau,\mu,\varphi) + \frac{\omega(\tau)}{4\pi}\int_0^{2\pi}\int_{-1}^{1} p(\tau,\mu',\mu,\varphi-\varphi')L(\tau,\mu',\varphi')\,d\mu' d\varphi', \qquad (1)$$

where τ is the optical depth, μ and φ are the cosine of the polar angle and the azimuth angle, respectively, ω is the single scattering albedo, while p is the single scattering phase function describing the angular distribution of the radiance after a single scattering event. The numerical solution of Eq. (1) based on the discrete ordinate method involves the following steps:

- The cosine azimuth expansion of the radiance field and the phase function which leads us to an equation for the azimuth component $L_m(\tau,\mu)$.
- Discretization of the radiance field in the μ -domain by considering N_{do} Gaussian points $\{\mu_i\}$ per hemisphere and corresponding weights $\{w_i\}$, where $i = 1,...,N_{do}$.
- Stratification of the inhomogeneous atmosphere as a system of N homogeneous layers: $\tau_1 < \tau_2 < ... < \tau_{N+1}$, where $\tau_1 = 0$ and $\tau_{N+1} = \tau_s$. A layer l is bounded above by the level τ_l and below by the level τ_{l+1}.

For layer l with the optical thickness $\bar{\tau}_l = \tau_{l+1} - \tau_l$ Eq. (1) is transformed into the system of ODEs (hereinafter for simplicity we omit azimuth index m):

$$\frac{d}{d\tau}\begin{bmatrix}\mathbf{i}^{\uparrow}(\tau)\\ \mathbf{i}^{\downarrow}(\tau)\end{bmatrix}=-\mathbf{A}_l\begin{bmatrix}\mathbf{i}^{\uparrow}(\tau)\\ \mathbf{i}^{\downarrow}(\tau)\end{bmatrix}+\mathbf{b}_l,\qquad \tau_l\le\tau\le\tau_{l+1}, \tag{2}$$

where $\left[\mathbf{i}^{\uparrow\downarrow}(\tau)\right]_i = L_m(\tau,\mp\mu_i)$, $i=1,...,N_{\text{do}}$, while $\mathbf{A}$ and $\mathbf{b}$ are the so called layer matrix and layer source vector, respectively (computational details can be found in [22]). The integral of Eq. (2) is

$$-\begin{bmatrix}\mathbf{i}_l^{\uparrow}\\ \mathbf{i}_l^{\downarrow}\end{bmatrix}+e^{\mathbf{A}_l\bar{\tau}_l}\begin{bmatrix}\mathbf{i}_{l+1}^{\uparrow}\\ \mathbf{i}_{l+1}^{\downarrow}\end{bmatrix}=\int_0^{\bar{\tau}_l}e^{\mathbf{A}_l t}\mathbf{b}_l(t)\,dt. \tag{3}$$

Next, to evaluate $\mathrm{e}^{\mathbf{A}_l\bar{\tau}_l}$, we make use of the singular value decomposition of the $\mathbf{A}$-matrix resulting in the following expression for the matrix exponential:

$$\mathrm{e}^{\mathbf{A}_l t}=\mathbf{V}_l\mathrm{e}^{\Lambda_l t}\mathbf{V}_l^{-1}, \tag{4}$$

where $\mathbf{V}$ is the eigenvector matrix and Λ is the eigenvalues matrix for the l th layer. Then, using Eq. (4) and Eq. (2) and rearranging the entries, we relate the radiances at the layer boundaries as follows:

$$\begin{bmatrix}\mathbf{i}_l^{\uparrow}\\ \mathbf{i}_{l+1}^{\downarrow}\end{bmatrix}=\begin{bmatrix}\mathbf{R}_l^{\uparrow} & \mathbf{T}_l^{\uparrow}\\ \mathbf{T}_l^{\downarrow} & \mathbf{R}_l^{\downarrow}\end{bmatrix}\begin{bmatrix}\mathbf{i}_l^{\downarrow}\\ \mathbf{i}_{l+1}^{\uparrow}\end{bmatrix}+\begin{bmatrix}\mathbf{Q}_l^{\uparrow}\\ \mathbf{Q}_l^{\downarrow}\end{bmatrix}, \tag{5}$$

where $\mathbf{R}_l^{\uparrow\downarrow}$ and $\mathbf{T}_l^{\uparrow\downarrow}$ are the reflection and transmission matrices, respectively, while $\mathbf{Q}_l^{\uparrow\downarrow}$ is the source term (see exact formulas in [22]).

In the case of a multilayer system, an equation similar to Eq. (5) can be derived by using the matrix operator method [23]. Indeed, for the l+1 th layer equation (5) takes the form

$$\begin{bmatrix}\mathbf{i}_{l+1}^{\uparrow}\\ \mathbf{i}_{l+2}^{\downarrow}\end{bmatrix}=\begin{bmatrix}\mathbf{R}_{l+1}^{\uparrow} & \mathbf{T}_{l+1}^{\uparrow}\\ \mathbf{T}_{l+1}^{\downarrow} & \mathbf{R}_{l+1}^{\downarrow}\end{bmatrix}\begin{bmatrix}\mathbf{i}_{l+1}^{\downarrow}\\ \mathbf{i}_{l+2}^{\uparrow}\end{bmatrix}+\begin{bmatrix}\mathbf{Q}_{l+1}^{\uparrow}\\ \mathbf{Q}_{l+1}^{\downarrow}\end{bmatrix}. \tag{6}$$

Using Eq. (5), we exclude $\mathbf{i}_{l+1}^{\downarrow}$ and $\mathbf{i}_{l+1}^{\uparrow}$ from Eq. (6) and obtain the equation for the larger layer encapsulating layers l and l+1:

$$\begin{bmatrix}\mathbf{i}_j^{+}\\ \mathbf{i}_{j+2}^{-}\end{bmatrix}=\begin{bmatrix}\mathbf{R}_{(j,j+1)}^{+} & \mathbf{T}_{(j,j+1)}^{+}\\ \mathbf{T}_{(j,j+1)}^{-} & \mathbf{R}_{(j,j+1)}^{-}\end{bmatrix}\begin{bmatrix}\mathbf{i}_j^{-}\\ \mathbf{i}_{j+2}^{+}\end{bmatrix}+\begin{bmatrix}\mathbf{Q}_{(j,j+1)}^{+}\\ \mathbf{Q}_{(j,j+1)}^{-}\end{bmatrix}, \tag{7}$$

where

$$\mathbf{R}_{(l,l+1)}^{\uparrow}=\mathbf{R}_l^{\uparrow}+\mathbf{T}_l^{\uparrow}\left(\mathbf{E}-\mathbf{R}_{l+1}^{\uparrow}\mathbf{R}_l^{\downarrow}\right)^{-1}\mathbf{R}_{l+1}^{\uparrow}\mathbf{T}_l^{\downarrow}, \tag{8}$$

$$\mathbf{R}_{(l,l+1)}^{\downarrow}=\mathbf{R}_{l+1}^{\downarrow}+\mathbf{T}_{l+1}^{\downarrow}\left(\mathbf{E}-\mathbf{R}_l^{\downarrow}\mathbf{R}_{l+1}^{\uparrow}\right)^{-1}\mathbf{R}_l^{\downarrow}\mathbf{T}_{l+1}^{\uparrow}, \tag{9}$$

$$\mathbf{T}^{\uparrow}_{(l,l+1)} = \mathbf{T}^{\uparrow}_{l}\left(\mathbf{E}-\mathbf{R}^{\uparrow}_{l+1}\mathbf{R}^{\downarrow}_{l}\right)^{-1}\mathbf{T}^{\uparrow}_{l+1}, \tag{10}$$

$$\mathbf{T}^{\downarrow}_{(l,l+1)} = \mathbf{T}^{\downarrow}_{l+1}\left(\mathbf{E}-\mathbf{R}^{\downarrow}_{l}\mathbf{R}^{\uparrow}_{l+1}\right)^{-1}\mathbf{T}^{\downarrow}_{l}, \tag{11}$$

$$\mathbf{Q}^{\uparrow}_{(l,l+1)} = \mathbf{Q}^{\uparrow}_{l} + \mathbf{T}^{\uparrow}_{l}\left(\mathbf{E}-\mathbf{R}^{\uparrow}_{l+1}\mathbf{R}^{\downarrow}_{l}\right)^{-1}\left(\mathbf{R}^{\uparrow}_{l+1}\mathbf{Q}^{\downarrow}_{l} + \mathbf{Q}^{\uparrow}_{l+1}\right), \tag{12}$$

$$\mathbf{Q}^{\downarrow}_{(l,l+1)} = \mathbf{Q}^{\downarrow}_{l+1} + \mathbf{T}^{\downarrow}_{l+1}\left(\mathbf{E}-\mathbf{R}^{\downarrow}_{l}\mathbf{R}^{\uparrow}_{l+1}\right)^{-1}\left(\mathbf{R}^{\downarrow}_{l}\mathbf{Q}^{\uparrow}_{l+1} + \mathbf{Q}^{\uparrow}_{l}\right), \tag{13}$$

$\mathbf{E}$ is the identity $N_{do}\times N_{do}$ matrix while lower indices in brackets refer to encapsulated layers. Note that the adding of the layer by going through Eqs. (8)-(13) requires 6 matrix inversions and 19 matrix multiplications.

For a multi-layered atmosphere, the reflection matrix of the entire atmosphere is computed recursively from the reflection and transmission matrices of each layer by using the adding algorithm. Starting from the top of the atmosphere, we combine the first and second layers to create a thicker single layer (a stack) with effective reflection and transmission matrices and source functions using Eqs. (8)-(13). The procedure is then repeated until the last layer is added to the stack. The application of the boundary conditions gives the radiance at the top of the atmosphere.

Two comments are in order:

1. After putting all the layers into the stack, an equation similar to Eq. (5) is obtained but with parameters for the whole stack. Taking the downwelling radiance $\mathbf{i}$ at the top of the medium and the upwelling radiance at the bottom of the medium from the boundary conditions, the reflected and transmitted radiances $\mathbf{i}^{\uparrow}_{l}$ and $\mathbf{i}^{\downarrow}_{l+1}$ can be readily found.
2. Even if we are interested only in the reflection matrix, the computations of both reflection $\mathbf{R}$ and transmission $\mathbf{T}$ matrices as well as the sources $\mathbf{Q}$ have to be performed to go though Eqs. (8)-(13).

2.2 Riccati equation formulation

The matrix Riccati equation can be derived through the propagator P_l [23, 24], such that

$$\begin{bmatrix}\mathbf{i}^{\uparrow}_{l+1}\\ \mathbf{i}^{\downarrow}_{l+1}\end{bmatrix} = \mathbf{P}_l\begin{bmatrix}\mathbf{i}^{\uparrow}_{l}\\ \mathbf{i}^{\downarrow}_{l}\end{bmatrix}. \tag{14}$$

From Eq. (5) it follows that

$$\mathbf{P}_l = \begin{bmatrix}\mathbf{T}^{\uparrow -1}_{l} & -\mathbf{T}^{\uparrow -1}_{l}\mathbf{R}^{\downarrow}_{l}\\ \mathbf{R}^{\uparrow}_{l}\mathbf{T}^{\downarrow -1}_{l} & \mathbf{T}^{\downarrow}_{l} - \mathbf{R}^{\uparrow}_{l}\mathbf{T}^{\uparrow -1}_{l}\mathbf{R}^{\downarrow}_{l}\end{bmatrix}. \tag{15}$$

On the other hand, from Eq. (2), it follows that

$$\frac{d}{d\tau}\mathbf{P}_l = \mathbf{A}_l\mathbf{P}_l. \tag{16}$$

Substituting Eq. (15) into Eq. (16), we obtain for the reflection matrix $\mathbf{R}_l^{\uparrow}$:

$$\frac{d}{d\tau}\mathbf{R}_l^{\uparrow} = \mathbf{b}_l + \mathbf{a}_l\mathbf{R}_l^{\uparrow} + \mathbf{R}_l^{\uparrow}\mathbf{a}_l + \mathbf{R}_l^{\uparrow}\mathbf{b}_l\mathbf{R}_l^{\uparrow}, \tag{17}$$

where $\mathbf{a}_l$ and $\mathbf{b}_l$ are the sub-matrices of $\mathbf{A}_l$:

$$\mathbf{A}_l = \begin{bmatrix} \mathbf{a}_l & \mathbf{b}_l \\ -\mathbf{b}_l & -\mathbf{a}_l \end{bmatrix}. \tag{18}$$

Eq. (17) can be generalized to the case when the optical properties are smoothly changing with the optical depth τ:

$$\frac{d}{d\tau}\mathbf{R}^{\uparrow}(\tau) = \mathbf{b}(\tau) + \mathbf{a}(\tau)\mathbf{R}^{\uparrow}(\tau) + \mathbf{R}^{\uparrow}(\tau)\mathbf{a}(\tau) + \mathbf{R}^{\uparrow}(\tau)\mathbf{b}(\tau)\mathbf{R}^{\uparrow}(\tau). \tag{19}$$

Then, by setting $\mathbf{R}^{\uparrow}(0) = 0$, Eq. (19) can be integrated numerically as an ODE.

3 Overview of ODE solvers

For the comparison we take the following ODE solvers: RK45, RK23, DOP853, BDF, LSODA.

1. RK45: the method of Dormand and Prince [25] of fifth order with embedded error estimator of order four. It uses six function evaluations per integration step.
2. RK23: explicit Runge-Kutta method [26] in which error is controlled using the second order method and it uses three function evaluation per integration step.
3. DOP853: embedded Runge-Kutta method of the eighth order with the dense output (seventh order) and step control [27]. A fifth order estimation with third order correction is used. It does twelve function evaluations per integration step.
4. BDF: implicit method with a variable step based on backward-differentiation formulas. This solver [28] has an order that automatically changes from 1 to 5.
5. LSODA: method which allows to automatically switch between stiff and nonstiff methods [29]. It has two regimes: Adams scheme and BDF scheme.

Note that in [30] the Riccati equation was derived for describing the transport of electrons in solids and the BDF algorithm was applied to solve it.

4 Numerical simulations

The SVD solver has been implemented in C++ and python 3.9. The implementation is based on the LAPACK and numpy libraries, respectively. The C++ implementation is about about 20 % faster than that in python. To evaluate the computation time accurately, the computations are repeated

100 times and the resulting elapsed time is divided by the number of repetitions. Computations are performed on a personal computer Intel Core i7-8700 CPU @ 3.20GHz (12 CPUs), 3.2GHz, 32GB RAM.

4.1 Homogeneous medium

To validate the solvers, we consider a homogeneous plane parallel layer. The optical thickness is 1, the single scattering albedo is 0.99, while the phase function is Henyey-Greenstein with the asymmetry parameter of 0.8. The phase function expansion coefficients are scaled following the delta-M procedure [31]. The computations are performed for the following values of N_{do}: 4, 8, 16 and 32. The result of computations is the reflection N_{do} by N_{do} matrix. The computation times of the solvers together with the mean and maximum relative errors (ε_{mean} and ε_{max}, respectively) are shown in Table 1. When computing ε_{mean}, the error is averaged across all elements of the reflection matrix.

Unlike the SVD method, which provides an accurate solution to equation (2), the ODE solvers are based on the approximate schemes of integration. In this regard, as the reference solution, we take the reflection matrix computed by the SVD method. Although, the SVD solver appears to be an order of magnitude faster than the ODE solvers, the latters provide an accurate solution within 0.1 % relative error in most cases. The RK23 solver gives the lowest accuracy, though being faster than DOP853, BDF and LSODA. The example of results obtained by the SVD solver and the ODE solvers for the N_{do} = 16, the optical thickness 1 and the normal angle of incidence are shown in Figure 1.

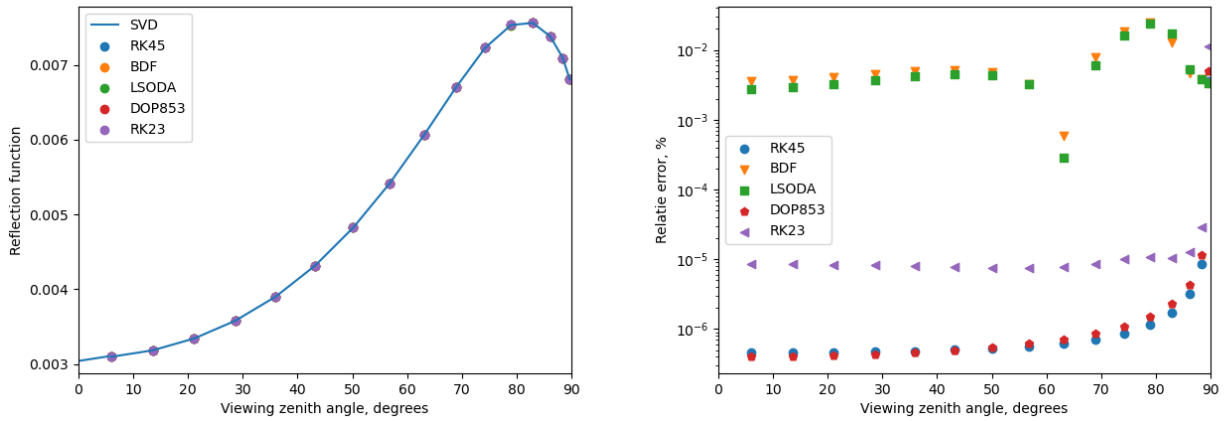

Figure 1: Comparison of results obtained by the SVD solver and the ODE solvers. (left) The reflection function for a normal incidence; (right) relative difference in percentage between the ODE solvers and the SVD solver.

Table 1: Computation time and the error of the SVD and ODE solvers. Homogeneous layer

	SVD	RK45	RK23	DOP853	BDF	LSODA

N_{do}	4					
Time, ms	0.2	2.0	3.0	3.9	8.9	3.0
ε_{mean}, %	—	0.05	0.02	7E-4	6.9E-3	1.2E-2
ε_{max}, %	—	0.45	0.45	0.45	0.46	0.45
N_{do}	8					
Time, ms	0.5	6.3	5.1	6.9	9.3	5.9
ε_{mean}, %	—	1.2E-5	6.54E-6	3.4E-5	3E-4	3E-4
ε_{max}, %	—	0.07	0.017	0.02	0.03	0.03
N_{do}	16					
Time, ms	1.0	29.9	24.9	28.9	36.9	51.9
ε_{mean}, %	—	4E-7	7.3E-6	4E-8	6E-5	5E-5
ε_{max}, %	—	0.75	2.23	1.0	0.03	0.03
N_{do}	32					
Time, ms	3.6	251	145	241	663	927
ε_{mean}, %	—	1E-10	1E-11	4E-10	2E-5	1E-5
ε_{max}, %	—	0.3	2.4	1.3	0.04	0.03

4.2 In-homogeneous medium

In this section we evaluate the performance of SVD and ODE solvers in the case of a inhomogeneous medium, namely, an example of a suspended absorbing particles in the air. The particles settle in the air making the single scattering albedo decreasing with the optical depth τ'. We parametrize the profile of the single scattering albedo as follows:

$$\omega(\tau') = \frac{e^{-b\tau'} - e^{-b\tau}}{1 - e^{-b\tau}}, \tag{20}$$

where b is a tuning parameter controlling the decreasing rate of the profile. The example of the profile of the single scattering albedo is shown in Figure 2.

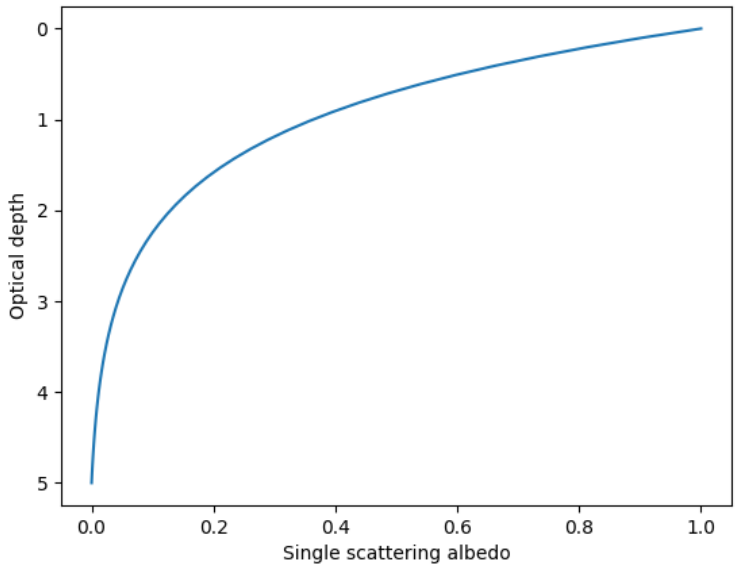

Figure 2: The single scattering albedo as a function of the optical depth.

The medium is spatially discretized into a set of N homogeneous layers of the optical thickness τ / N each. The single scattering albedo of each sublayer $\hat{\omega}$ is taken as the integral-average value across the optical depth, namely,

$$\hat{\omega}_l = \int_{\tau_l}^{\tau_{l+1}} \omega(\tau') d\tau'. \tag{21}$$

To make the comparison consistent, the stratified system is given as input to the ODE solvers. The results of comparison are shown in Tables 2-4. The resutls are shown for those values of *N*, at which the relationship in the computation time between SVD and at least one ODE solver changes. Note, that in practise, to evaluate the required number of layers, one could iteratively increase the spatial discretization until the solutions at two consequent iterations differ by less than a given threshold. A detailed analysis of the errors associated with the representation of an inhomogeneous medium as a system of homogeneous layers can be found in [32–33]. Discretization error is not considered in this work.

Table 2: Computation time and the error of the SVD and ODE solvers for an in-homogeneous layer with $\tau = 0.1$

	SVD	RK45	RK23	DOP853	BDF	LSODA	N layers
N_{do}	4						
*Time, ms	0.65	0.94	2.19	**0.62**	1.26	0.78	1
	1.92	**0.78**	2.34	**0.78**	**1.17**	**0.78**	2
	2.34	**1.2**	**1.95**	**0.78**	**1.56**	**0.78**	5

ε_{mean}, %	—	0.3	0.3	0.3	0.3	0.4	—
ε_{max}, %	—	0.4	0.4	0.4	0.4	0.5	—
N_{do}	8						
*Time, ms	1.47	**1.11**	4.23	**1.09**	1.87	**0.94**	2
	3.13	**1.25**	4.03	**1.09**	**1.87**	**0.95**	4
	4.7	**1.32**	**4.07**	**1.25**	**1.84**	**1.1**	6
ε_{mean}, %	—	0.004	0.01	0.004	0.001	0.13	—
ε_{max}, %	—	0.04	0.07	0.02	0.002	0.53	—
N_{do}	16						
*Time, ms	3.12	**2.43**	22.01	18.75	4.69	3.73	2
	15.63	**3.12**	21.87	17.18	**3.12**	**3.12**	10
	21.87	**3.12**	**20.3**	**18.75**	**4.69**	**3.12**	15
ε_{mean}, %	—	0.001	0.011	0.008	0.00008	0.012	—
ε_{max}, %	—	0.24	0.097	0.037	0.018	2.34	—
N_{do}	32						
*Time, ms	18.75	20.31	303.34	307.27	20.42	**15.62**	3
	24.99	**21.29**	291.91	305.54	**21.52**	**17.3**	5
	324.16	**20.31**	**294.28**	**315.29**	**23.54**	**12.5**	60
ε_{mean}, %	—	0.002	0.006	0.005	0.00008	0.007	—
ε_{max}, %	—	2.2	0.04	0.04	0.07	6.7	—

Table 3: The same as in Table 2, but for $\tau = 1$

	SVD	RK45	RK23	DOP853	BDF	LSODA	N layers
N_{do}	4						
*Time, ms	2.34	2.34	3.71	**1.95**	**2.26**	**1.56**	4
	2.4	**1.95**	4.23	**1.56**	**2.34**	**1.79**	5
	4.69	**2.15**	**3.91**	**1.59**	**2.34**	**1.56**	9
ε_{mean}, %	—	0.2	0.19	0.2	0.19	0.2	—
ε_{max}, %	—	0.46	0.47	0.45	0.46	0.45	—
N_{do}	8						
*Time, ms	4.21	5.47	5.94	5.75	5.73	**3.93**	6
	5.73	**5.49**	6.43	**5.66**	6.53	**3.83**	8
	7.81	**5.43**	**6.15**	**5.49**	**6.04**	**3.83**	10
ε_{mean}, %	—	0.002	0.01	0.01	0.001	0.004	—

ε_{max}, %	—	0.08	0.04	0.03	0.03	0.2	—
N_{do}	16						
*Time, ms	15.87	24.23	21.51	58.61	28.97	**15.18**	11
	31.48	**21.87**	**25.1**	59.13	**24.99**	**15.73**	20
	60.94	**21.55**	**23.43**	**54.78**	**23.18**	**15.62**	37
ε_{mean}, %	—	0.003	0.009	0.009	0.005	0.01	—
ε_{max}, %	—	0.75	0.03	0.03	1.02	2.2	—
N_{do}	32						
*Time, ms	114.4	171.5	348.9	684	158.65	**101.3**	18
	335.9	**171.3**	366.9	692.1	**161.6**	**098.2**	60
	699.7	**173.7**	**348.2**	**670.7**	**159.9**	**101.1**	136
ε_{mean}, %	—	0.0003	0.01	0.008	0.001	0.002	—
ε_{max}, %	—	0.3	0.04	0.03	1.3	2.4	—

Table 4: The same as in Table 2, but for $\tau = 10$

	SVD	RK45	RK23	DOP853	BDF	LSODA	N layers
N_{do}	4						
*Time, ms	4.7	11.7	6.3	**3.5**	10.9	7.8	9
	8.6	11.6	**6.2**	**3.5**	11.4	**7.97**	17
	12.3	**11.4**	**6.3**	**3.5**	**10.9**	**8.2**	25
ε_{mean}, %	—	0.07	0.05	0.03	0.06	0.08	—
ε_{max}, %	—	0.12	0.1	0.055	0.12	0.2	—
N_{do}	8						
*Time, ms	9.4	46.6	**8.2**	12.9	39.9	29.7	12
	14.1	46.8	**8.4**	**12.5**	39.6	29.7	20
	48.3	**46.2**	**8.2**	**12.9**	**39.7**	**29.6**	65
ε_{mean}, %	—	0.003	0.02	0.03	0.001	0.01	—
ε_{max}, %	—	0.12	0.04	0.07	0.04	0.6	—
N_{do}	16						
*Time, ms	34.4	232.8	**25.1**	97.4	200.7	144.4	20
	120.8	226.9	**27.09**	**96.6**	196.5	140.4	80
	240.9	**225.5**	**26.6**	**102.85**	**194.1**	**141.3**	120
ε_{mean}, %	—	0.001	0.01	0.03	0.002	0.004	—
ε_{max}, %	—	0.3	0.03	0.07	0.5	0.8	—

N_{do}	32						
*Time, ms	508.8	1670.2	**377.6**	960.5	1380.3	935.1	100
	1025.4	1677.04	**390.4**	**969.98**	1392.7	**944**	200
	1672.2	**1665.3**	**379.6**	**962.5**	**1389.1**	**943.7**	340
ε_{mean}, %	—	0.002	0.02	0.03	0.00006	0.0001	—
ε_{max}, %	—	1.8	0.04	0.07	0.06	0.1	—

Notes: **Bold** indicates the times of computation of ODE solvers, which are faster than SVD method.

5 Conclusions

In this paper we have analyzed the efficiency of ODE solvers for finding the reflection matrix by solving the one-dimensional RTE. As a reference solution, we take that based on the singular value decomposition method.

For a homogeneous medium, the SVD solver is an order of magnitude faster than the considered ODE solvers. Nevertheless, the ODE solver provide accurate solution with the order of relative difference is about 0.1 %. For the inhomogeneous medium, the efficiency of ODE solvers increases the number of layers increases. However, the more discrete ordinates are, the larger is the number of layers at which the ODE solvers outperform the SVD solver. For instance, for $N_{do} = 4$ and $N_{do} = 32$, it takes place at 4 and 18 layers, respectively. Also we note that the number of layers at which the ODE solvers become more efficient increases with the optical thickness of the medium.

From our point of view, the main benefit of ODE solvers is a dynamic detection of the required spatial discretization of the medium. They do not require computations of the transmission functions and application of the matrix operator method. Besides, if the optical properties are vertically inhomogeneous, the ODE solvers internally fit the appropriate step of integration to satisfy the accuracy requirements. Another application of ODE solvers is the computations of the lookup tables for a set of layer optical thicknesses. While the SVD method can reuse only the eigenvalue decomposition results for such computations, the ODE solvers automatically provide the solution for the required set of layer optical thicknesses. A thorough evaluation of this case will be a subject of our future papers.

References

1. S. Twomey and H. Jacobowitz and H. B. Howell. Matrix Methods for Multiple-Scattering Problems. *J. Atmos. Sci.*, 23(3):289–298, 1966.

2. Sobolev, V. V. and ter Haar, D. *Light Scattering in Planetary Atmospheres*. Pergamon Press, 1975.

3. James E. Hansen and Larry D. Travis. Light scattering in planetary atmospheres. *Space Science Reviews*, 16(4):527–610, 1974.

4. William M. Irvine. Multiple scattering in planetary atmospheres. *Icarus*, 25(2):175–204, 1975.

5. Lenoble, J. *Radiative Transfer in Scattering and Absorbing Atmospheres: Standard Computational Procedures* of Studies in geophysical optics and remote sensing. A. Deepak, 1985.

6. Budak, V.P. and Klyuykov, D.A. and Korkin, S.V. Convergence acceleration of radiative transfer equation solution at strongly anisotropic scattering. In Kokhanovsky, A A, editors, *Light scattering reviews*, pages 147–203. Springer Berlin Heidelberg, 2010.

7. Afanas'ev, V. P. and Efremenko, D. S. and Lubenchenko, A. V. On the application of the invariant embedding method and the radiative transfer equation codes for surface state analysis. In Kokhanovsky, A.A., editors, *Light Scattering Reviews 8*, pages 363–423. Springer Science + Business Media, 2013.

8. Rozanov, V.V. and Rozanov, A.V. and Kokhanovsky, A.A. and Burrows, J.P. Radiative transfer through terrestrial atmosphere and ocean: Software package SCIATRAN. *Journal of Quantitative Spectroscopy and Radiative Transfer*, 133:13–71, 2014.

9. Rogovtsov, N.N. and Borovik, F. Application of general invariance relations reduction method to solution of radiation transfer problems. *Journal of Quantitative Spectroscopy and Radiative Transfer*, 183:128–153, 2016.

10. Barry D. Ganapol and Japan Patel. Matrix Riccati Equation Solution of the 1D Radiative Transfer Equation. *Journal of Computational and Theoretical Transport*, 50(5):297–327, 2020.

11. Wick, G. C. über ebene Diffusionsprobleme. *Zeitschrift für Physik*, 121(11-12):702–718, 1943.

12. Chandrasekhar, S. *Radiative Transfer*. Dover Publications, Inc., New York, 1950.

13. Knut Stamnes. The theory of multiple scattering of radiation in plane parallel atmospheres. *Rev. Geophys.*, 24(2):299, 1986.

14. P. C. Waterman. Matrix-exponential description of radiative transfer. *Journal of the Optical Society of America*, 71(4):410, 1981.

15. Efremenko, Dmitry and Doicu, Adrian and Loyola, Diego and Trautmann, Thomas. Acceleration techniques for the discrete ordinate method. *Journal of Quantitative Spectroscopy and Radiative Transfer*, 114:73–81, 2013.

16. Efremenko, Dmitry S. and Loyola, Diego G. and Doicu, Adrian and Spurr, Robert J D. Multi-core-CPU and GPU-accelerated radiative transfer models based on the discrete ordinate method. *Computer Physics Communications*, 185(12):3079–3089, 2014.

17. Efremenko, D S and Loyola, D and Spurr, R J D and Doicu, A. Acceleration of radiative transfer model calculations for the retrieval of trace gases under cloudy conditions. *J Quant Spectrosc Radiat Transfer*, 135:58–65, 2014.

18. Ambarzumian, V.A. Diffuse reflection of light by a foggy medium. *Dokl. Akad. Nauk SSSR*, 38:229-232, 1943.

19. Bellman, R. and Kalaba, R. and Wing, G.M. Invariant imbedding and mathematical physics-I: Particle processes. *J. Math. Phys.*, 1:280-308, 1960.

20. Piotr J. Flatau and Graeme L. Stephens. On the fundamental solution of the radiative transfer equation. *J. Geophys. Res.*, 93(D9):11037, 1988.

21. Nakajima, T and Tanaka, M. Matrix formulations for the transfer of solar radiation in a plane-parallel scattering atmosphere. *J Quant Spectrosc Radiat Transfer*, 35(1):13–21, 1986.

22. Efremenko, Dmitry and Kokhanovsky, Alexander. *Foundations of Atmospheric Remote Sensing*. Springer, 2021.

23. V P Budak and D S Efremenko and O V Shagalov. Efficiency of algorithm for solution of vector radiative transfer equation in turbid medium slab. *J. Phys.: Conf. Ser.*, 369:012021, 2012.

24. Viktor P. Afanas'ev and Alexander Yu. Basov and Vladimir P. Budak and Dmitry S. Efremenko and Alexander A. Kokhanovsky. Analysis of the Discrete Theory of Radiative Transfer in the Coupled "Ocean–Atmosphere" System: Current Status, Problems and Development Prospects. *Journal of Marine Science and Engineering*, 8(3):202, 2020.

25. Dormand, J.R. and Prince, P.J. A family of embedded Runge-Kutta formulae. *Journal of Computational and Applied Mathematics*, 6:19-26, 1980.

26. P. Bogacki and L.F. Shampine. A 3(2) pair of Runge - Kutta formulas. *Applied Mathematics Letters*, 2(4):321–325, 1989.

27. E. Hairer and G. Wanner and S.P. Norsett. *Solving Ordinary Differential Equations I:*

Nonstiff problems. Springer Berlin Heidelberg, 1993.

28. L. F. Shampine and M. W. Reichelt. THE MATLAB ODE SUITE. *SIAM J. SCI. COMPUTE.*, 18:1–22, 1997.

29. Linda Petzold. Automatic Selection of Methods for Solving Stiff and Nonstiff Systems of Ordinary Differential Equations. *SIAM Journal on Scientific and Statistical Computing*, 4(1):136–148, 1983.

30. Afanas'ev, V.P. and Efremenko, D.S. and Kaplya, P.S. Analytical and numerical methods for computing electron partial intensities in the case of multilayer systems. *Journal of Electron Spectroscopy and Related Phenomena*, 210:16–29, 2016.

31. Wiscombe W.J. The Delta–*M* Method: Rapid Yet Accurate Radiative Flux Calculations for Strongly Asymmetric Phase Functions. *Journal of the Atmospheric Sciences*, 34:1408-1422, 1977.

32 Minzheng Duan, Qilong Min, and Knut Stamnes. Impact of vertical stratification of inherent optical properties on radiative transfer in a plane-parallel turbid medium. Opt. Express 18: 5629-5638, 2010.

33. Yi-Ning Shi, Feng Zhang, Ka Lok Chan, Thomas Trautmann, and Jiangnan Li, Multi-layer solar radiative transfer considering the vertical variation of inherent microphysical properties of clouds, Opt. Express 27: A1569-A1590 , 2019.